JOURNAL OF SPACECRAFT AND ROCKETS
Vol. 30, No. 3, May–June 1993

High Temporal Resolution Velocity Estimates from a Wind Profiler

Timothy L. Wilfong*
Universities Space Research Association, Huntsville, Alabama 35806
Steve A. Smith†
NASA Marshall Space Flight Center, Huntsville, Alabama 35812
and
Robert L. Creasey‡
Universities Space Research Association, Huntsville, Alabama 35806

Existing techniques for rejecting spurious data in single-cycle wind profiles employ a consensus average method to several profiles. This technique sometimes fails and also severely limits temporal resolution. The authors find by first applying a median filter to three successive single-cycle (3 min) spectral data and then guiding the velocity calculation by a first guess, it is possible to extract high-quality wind profiles at 3-min intervals. For support to launch operations, it is critical the wind-profile data be correct. The authors introduce an interactive quality control methodology in which the median spectral data are overlaid with the computed velocity profile. Two test cases are presented.

Nomenclature

F_n	= Nyquist frequency, s^{-1}
NCOH	= number of pulses averaged to form a coherent average
NFFT	= number of points in the FFT
PRP	= pulse repetition period, s
V_{h45}	= horizontal velocity at azimuth 45 deg, m/s
V_{h135}	= horizontal velocity at azimuth 135 deg, m/s
V_{r45}	= radial velocity in the 45-deg azimuth beam, m/s
V_{r135}	= radial velocity in the 135-deg azimuth beam, m/s
ΔF	= frequency resolution of a power spectrum, s^{-1}
ΔV	= velocity resolution of the profiler, m/s
λ	= wavelength of the radar signal, m

Introduction

As part of the effort to improve and streamline winds aloft inputs to the day of launch evaluations, NASA is transitioning wind profiling radar technology to operations. Existing techniques routinely used in wind-profiling technology limit the temporal resolution and allow some erroneous data to pass unchecked.

Wind-profiling radars depend on scattering from small variations in the radio refractive index of air. Most electromagnetic energy incident upon small spatial variations of the radio refractive index is propagated in the forward direction. Only a very small amount is backscattered. The amount of backscatter from a given volume of air is proportional to the amplitude of variations in refractive index—commonly quantified as the refractive-index structure function. In addition to refractive-index irregularities, scattering occurs from hydrometers, airplanes, and other airborne objects. These generally produce unwanted or spurious echoes that complicate the wind computation process and often introduce the errors mentioned above. Existing methods for rejecting spurious data generally ignore noise problems in extracting a wind profile and then apply a consensus average technique to several profiles—usually ten or so—to remove unwanted noise and spurious winds. This technique sometimes fails and also limits temporal resolution. A key element in the operational transition, therefore, is the development of a methodology to extract complete wind profiles at frequent intervals as well as provide for quality control of those wind profiles before distribution. This paper describes the technique being implemented.

Received Nov. 22, 1991; presented as Paper 92-0719 at the AIAA 30th Aerospace Sciences Meeting, Reno, NV, Jan. 6-9, 1992; revision received April 27, 1992; accepted for publication May 3, 1992.

*Research Associate, 4950 Corporate Drive, Suite 100. Member AIAA.
†Staff Scientist, Space Sciences Lab.
‡Research Associate, 4950 Corporate Drive, Suite 100.

Operating Characteristics

The NASA prototype wind profiler operates at 49.25 MHz with an average power-aperture product of 10^8 Wm^2. A wide range of parameter settings provides complete flexibility in the radar operating characteristics. Nominally an 8-μs pulse consisting of 1-ms code elements is used to yield a range resolution of 150 m over 112 gates. The lowest gate is nominally set to 2 km giving a maximum altitude of 18.6 km.

The antenna is a phased array of coaxial-colinear elements which the radar uses to create three beams—one vertical (mode 3) and two orthogonal beams 15 deg off the zenith on azimuths of 135 deg (mode 1) and 45 deg (mode 2). The pulse repetition period (*PRP*) is 160×10^{-6} s. A cycle is completed by integrating in each beam for 1 min. In modes 1 and 2, the radar real-time processor coherently integrates 320 pulses (*NCOH*). A Fast Fourier Transform (FFT) is then applied to 256 of these points (*NFFT*) to produce a spectral estimate. Four sets of spectral estimates are then incoherently averaged to produce the final 1-min estimates. In mode 3 (vertical), only one spectral estimate is formed over the entire minute after coherently averaging 1400 pulses.

If *NCOH* is used to refer to the number of individual pulse returns averaged, the maximum frequency detectable (the Nyquist frequency) is

$$F_n = 1/\{2(PRP)(NCOH)\} \tag{1}$$

The frequency resolution of the power spectrum is the inverse of the time required to gather the data for an FFT calculation

$$\Delta F = 1/\{(NFFT)(NCOH)(PRP)\} \tag{2}$$

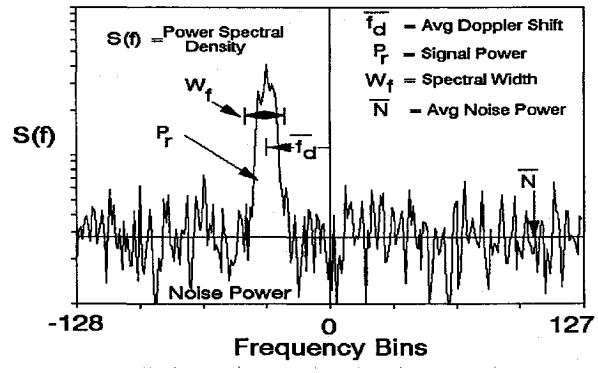

Fig. 1 Model power spectrum.

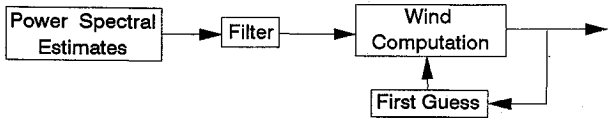

Fig. 2 Wind-profile calculation using a first guess.

Employing the Doppler frequency to velocity relationship ($F = 2V/\lambda$), we can compute the maximum unaliased velocity and the velocity resolution from Eqs. (1) and (2)

$$V_{\max} = \lambda/4(NCOH)(PRP) \tag{3a}$$

$$\Delta V = \lambda/2(NFFT)(NCOH)(PRP) \tag{3b}$$

where $V_{\max}$ and ΔV refer to limits—which can be positive or negative. Thus, in modes 1 and 2 a radial velocity resolution of 0.232 m/s is achieved over the range ± 29.6 m/s. In other words each bin in the Doppler shift spectrum is 0.232 m/s wide. In mode 3 the radial velocity resolution is 0.05 m/s over the range ± 6.7 m/s.

At present, the system computes velocity estimates using software delivered by TYCHO Technology, the manufacturer. Three-minute wind-profile estimates are computed from the single-cycle spectral data using the so-called moment method. Simply stated, the radial velocity computation finds the largest spectral peak at each gate and then integrates over the signal power down to the noise level to estimate the Doppler frequency shift which, in turn, corresponds to a radial velocity estimate V_r. Figure 1 shows a model power spectrum.

The velocity from the vertical beam V_w can be used directly while the radial velocity estimates in each of the oblique beams are converted to horizontal velocities, using the relation

$$V_{h45} = V_{r45}/\sin(15 \text{ deg}) \tag{4a}$$

$$V_{h135} = V_{r135}/\sin(15 \text{ deg}) \tag{4b}$$

where the subscripts 45 and 135 refer to the oblique beam pointing azimuth. To combine the radial velocities into a vector wind, one assumes the atmosphere is horizontally homogeneous (no significant variations in the horizontal) and stationary (no significant variations in time) over the areas covered by the radar beams during the 3-min integration time. In locations or situations where there is a significant large scale vertical velocity—for example, near mountains in a standing wave situation—the vertical velocity contributes significantly to the radial velocities in the oblique beams; and therefore, V_{r45} and V_{r135} in Eq. (4) must be corrected by subtracting $V_W \cos(15 \text{ deg})$ to compute accurate horizontal velocities. Such conditions are rare in central Florida and the two oblique velocities are computed without correction. Typically, vertical velocities large enough to adversely affect the profiler horizontal velocities usually occur in strongly convective situations—in which case the horizontal homogeneity assumption is also suspect. Vertical velocity statistics are, therefore, used as a quality indicator. The horizontal winds obtained in Eq. (4) are combined to form the standard meteorological north/south v and east/west u horizontal velocity vector estimates using

$$u = -V_{h135} \sin(135) - V_{h45} \cos(45) \tag{5a}$$

$$v = -V_{h45} \cos(45) + V_{h135} \sin(135) \tag{5b}$$

Single-cycle wind estimates (i.e., 3-min wind estimates) are quality controlled by applying a consensus average. After ten cycles, the 30-min consensus is formed at each of the 112 gates by searching the ten computed radial velocities for four or more observations whose differences are less than 2 m/s (radial velocity). If four or more observations are found, they are all averaged. Consensus radial velocities thus obtained are then used to form the horizontal wind vector which is reported to the Eastern Space and Missile Center's Meteorological Information Data Display System (MIDDS).

Although the consensus average coupled with the wind computation algorithm discussed above performs acceptably for many applications, significant problems arise for launch support operations. In particular, the technique may report erroneous winds or fail to compute a consensus at all. Furthermore, the 30-min consensus is roughly equivalent to block averaging the date; therefore, small-scale wind fluctuations are severely attenuated. For optimal launch support, complete and accurate profiles at high temporal resolution are essential. Complete, quality controlled profiles should be available at 15-min increments as a minimum.

Our approach in developing an improved velocity extraction technique was to begin as early in the data processing cycle as practicable. Essentially, we have begun with the power spectral data that are the output of the real-time radar processor. Unfortunately these data are not yet readily available in real time. Spectral data output must be recorded on magnetic tape and processed offline. Thus, although the techniques presented here were developed with the goal of real-time implementation, minor modifications and enhancements will be necessary. Final tailoring of the technique will be accomplished by the NASA Applied Meteorology Unit located in the Cape Canaveral Forecast Facility.

Review and analysis of many profiler spectral samples, when the single-cycle velocity computation produces an erroneous wind, have shown there is a weaker but identifiable atmospheric signal in the radar spectral data. More sophisticated algorithms are required to take full advantage of the technology.

Improved Velocity Computation Methodology

Extracting a wind profile from spectra is envisioned as a two step process. First, spectra are filtered to reject spurious echoes and improve signal-to-noise ratios. Second, the velocity computation proceeds on the filtered spectra guided by a first guess. Figure 2 shows a schematic of the process. Of course, a key element is the formulation of the first guess. To begin the process, the first guess may be determined by any means available such as a balloon sounding or the profiler itself.

The Median Filter

Our evaluations indicate a median filter applied to successive spectral estimates retains many advantages of a simple arithmetic mean while maintaining superior rejection of transient interference such as airplanes.[2] Of course the median filter must be applied with some care since, in addition to transient interference, atmospheric signals with time scales on the order of half of the median filter time scale or less will also be rejected. We do not routinely apply a median filter to the

vertical beam spectra since it is generally desirable to observe short time-scale variations in vertical velocities. As mentioned earlier, the vertical data are used only as a quality indicator. We shall confine the following discussions to the oblique beam spectra.

Figure 3 shows the results of a five-point median applied to a single mode 2 gate centered at 14,150 m. These data were gathered during the launch of STS 37 on April 5, 1991. Figure 3 also shows a persistent problem present until the receiver was repaired in June 1991. Whenever a spectral peak was produced by either an atmospheric signal or some spurious return, a second peak usually reduced in amplitude was mirrored on the opposite side of zero Doppler shift from the actual peak. In Fig. 3, for example, the atmospheric peak is located at about -8 m/s, while the artifact is located at about $+8$ m/s. The artifact nominally presented a problem only when the velocity in a given beam was within a few meters per second of zero. Since the weighted velocity computation currently integrates down to the computed noise level, the artifact was encountered before the noise level was reached and was included in the weighted average. Thus the velocity was reported erroneously as nearly zero. The velocity integration constraint to be described later has proven effective in dealing with such problems.

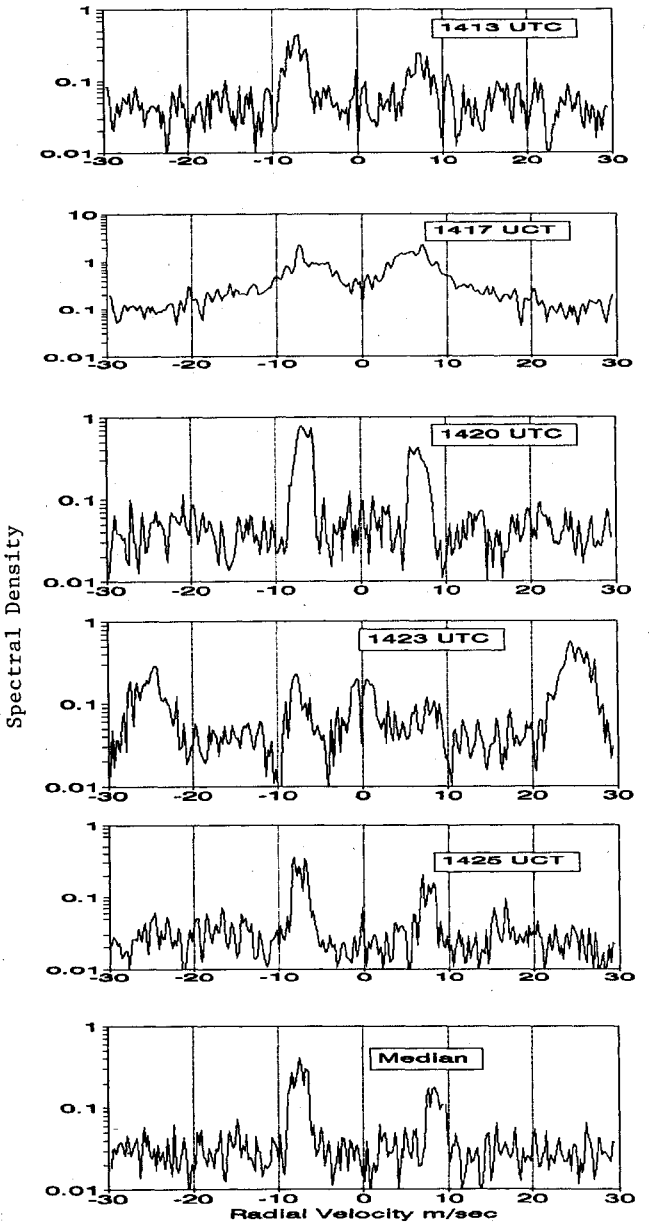

Fig. 3 Five-point median filter applied to successive spectral measurements taken on April 5, 1991 from gate 81, mode 2.

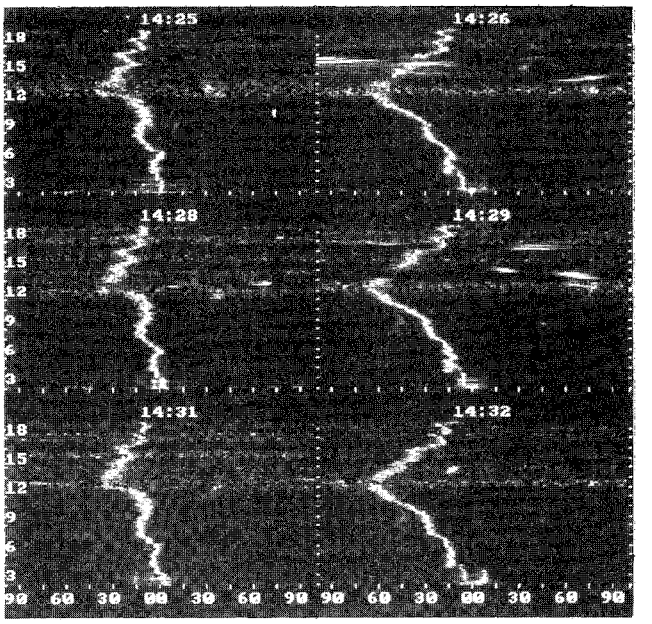

Fig. 4 December 6, 1990 oblique beam power spectral profiles. Profiles on the left are from mode 1 (135-deg azimuth) and those on the right are mode 2 (45-deg azimuth). UCT times are shown above each profile. Altitudes shown on the ordinate are in kilometers. Abscissae are labeled with the equivalent horizontal wind speed in meters/second.

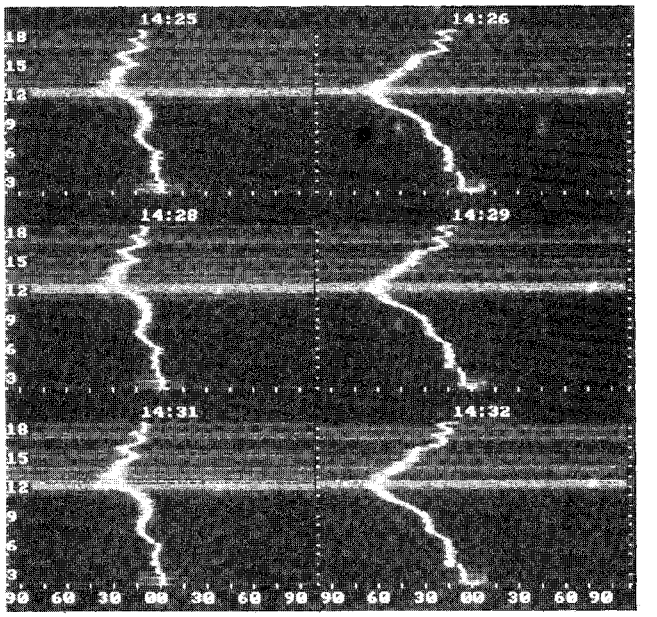

Fig. 5 Three-point median filter applied to data in Fig. 4.

Spectral Data Display

To develop a technique with a potential application to the real-time launch environment, we first developed an efficient and meaningful way to look at the spectral data. Spectral plots are usually presented in a graphical form such as Fig. 3. Using such a display it is not possible to quickly examine entire profiles. To display complete profiles of spectra, we convert each power spectrum to a color spectrum. Figure 4 shows such a display using gray scales rather than color. To produce this display, each power spectrum is scaled by its largest member and displayed using

$$\text{Color}(f) = (\text{Full scale}) * \log(1 + 9S(f)/S_{\max}) \qquad (6)$$

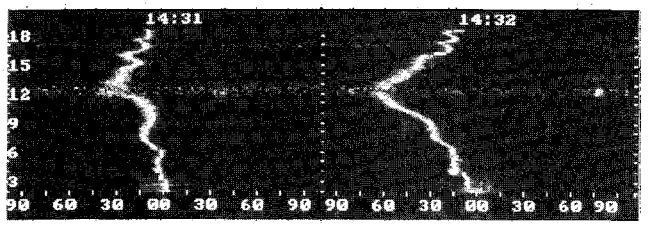

Fig. 6 Three-point median filter and noise removal applied to data in Fig. 4.

where $S(f)$ refers to the power spectral density estimates, S_{max} is the maximum density in the spectrum, and full scale refers to the maximum number of colors or gray scales—256 in these examples. Color thus varies from zero to full scale. At gates where there is very little signal, the power spectral data are all close in magnitude. Thus, as a result of scaling the data at each gate by the largest member, low signal-to-noise ratios show up as elevated gray scales (i.e., a dark region).

Rather than radial velocity or Doppler shift, the abscissae in Fig. 4 are labeled with the horizontal velocity corresponding to the Doppler shift. This particular case demonstrates a problem often encountered in jet stream situations. Near the center of the jet stream (approximately 12 km), where the temperature lapse rate is approximately adiabatic, the refractive-index structure function is often very small resulting in poor scatter and very low signal-to-noise ratios. As discussed above, this is evidenced by elevated (darker) gray scales.

Figure 5 shows the effect of a three-point median filter on the data in Fig. 4. Spurious echoes, possibly from aircraft, are removed and signal-to-noise is improved. Near the center of the jet stream, however, there are still low signal-to-noise ratios.

To improve the display further, we subtract the noise level from $S(f)$ and again use Eq. (6) to display the results. Figure 6 shows the results of such an application to the median spectra shown in Fig. 5. This display forms the basis for quality control of wind profiles in an operational setting.

Formulation of the First Guess

The first-guess technique is an extremely powerful method for reducing the probability of a false detection; however, the formulation of the first guess must be done with care. Green[2] employed a velocity tracing technique, beginning with the lowest gates and working upward searching for a radar echo over a range based on a "reasonable shear." This technique depends completely upon the initial detection/calculation being correct. In addition, such a technique has a high probability of failure if a region is encountered where no detectable signal is present which often happens in the core of a strong jet stream.

Our approach to the first-guess formulation is to use "prior knowledge" of the wind profile coupled with interactive quality control. At each 3-min cycle, the first guess for the wind profile is just the previous wind profile. To compute the wind at each gate, a search is done of the spectral bins close to the bin defined by the first guess to find the maximum signal point. For nominal 3-min cycle data this search is confined to ± 3 bins, but can be interactively expanded.

If no detectable signal is found (signal-to-noise ratios less than -15 dB), the first guess is merely propagated for a short time and a quality control counter is incremented for each successive propagation. If this condition persists for a period of time—nominally 15 min—the first guess is modified slightly at the gates with low signal. The profile is smoothed vertically using a five-point running mean and the averaged points replace the propagated first guess where the signal drop out is persistent.

This technique can be led astray if there are spurious signals very close to the first guess. Although such an effect can occur virtually at any level, it is a recurring situation in the lowest gates where ringing is sometimes a problem. To overcome this complication, the lowest gates are handled differently. Below a selectable gate (usually ten), downward velocity tracing is used. The technique (hereafter referred to as the low gate procedure) begins with the first guess described above and works its way down the profile using the velocity computed at the previous gate as a first guess. The first guess window is constrained using a reasonable shear—usually ± 6 bins. In some cases, we have found that this technique will produce erroneous winds. However, since the first guess is never propagated in time at these lower gates, the effect is short lived and, perhaps more importantly, the problem is immediately obvious in the display.

Velocity Calculation

To compute radial velocity at each gate, we first apply the method of Hildebrand and Sekhon[3] as discussed by Clark and Carter[1] to determine the noise level in the filtered spectrum. Integration proceeds from the maximum signal point to the noise level on either side or until a specified number of bins has been used on either side. To quantify this integration

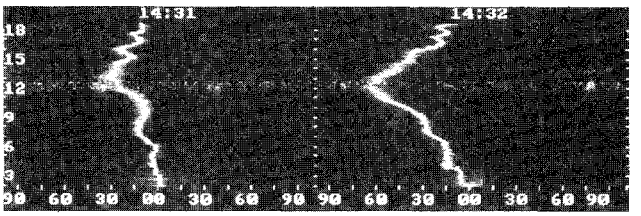

Fig. 7 Data from Fig. 6 with computed velocity profiles overlaid.

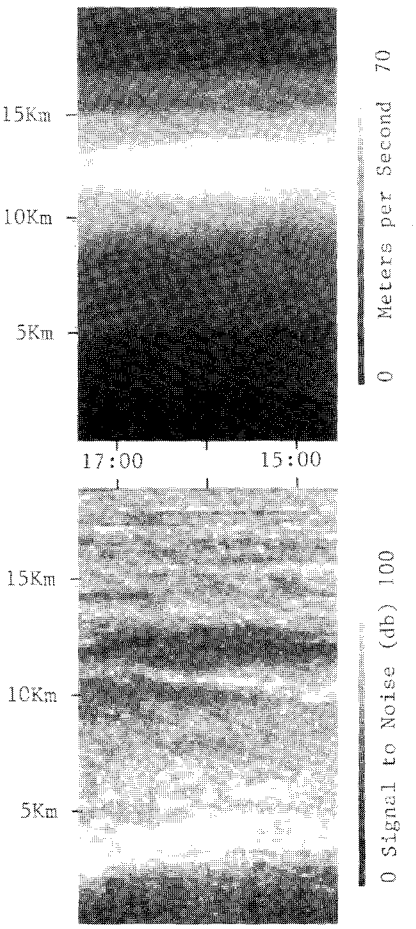

Fig. 8 Wind-speed (top) and signal-to-noise profiles from Dec. 6, 1990. Data are from 14:06 to 17:33 UCT. Time progresses from right to left. Signal-to-noise ratios have been corrected for range.

constraint, we examined spectral widths in numerous data sets. The spectral width is usually on the order of 0.4–0.6 m/s (radial velocity) in the oblique beams—about 3 bins wide. This value corresponds to the standard deviation of velocities in the signal spectrum. We have chosen the integration constraint to accommodate a large variance in the signal. Up to 5 bins on either side of the signal maximum are used in the integration—no more than 11 bins total. Again this constraint can be interactively changed.

Quality Control

We have employed the technique described here to process several sample data sets of durations from 3 to 8 h. In these cases, the process has not required correction or any manual interaction other than the formulation of the first guess. We expect, however, the process will require occasional interaction by an operator when processing continuous data. During launch support operations the process will require monitoring and quality control.

The technique behind the production of Fig. 6 is the basis of our formulation of a prototype procedure to be employed to support operations. Visual examination of spectral data displayed in this way provide an excellent estimate of the velocity profile. By overlaying the computed velocity profiles, any significant errors or areas of uncertainty become apparent. Figure 7 shows the results of this procedure applied to the median data shown in Fig. 6. In gray scale displays such as this, the profile is virtually not distinguishable from the spectral data—unless there is an error. In Fig. 7, the brightness (or blackness) of the spectral profile is slightly suppressed so that the velocity profile can be more easily seen. This procedure is not required in color displays.

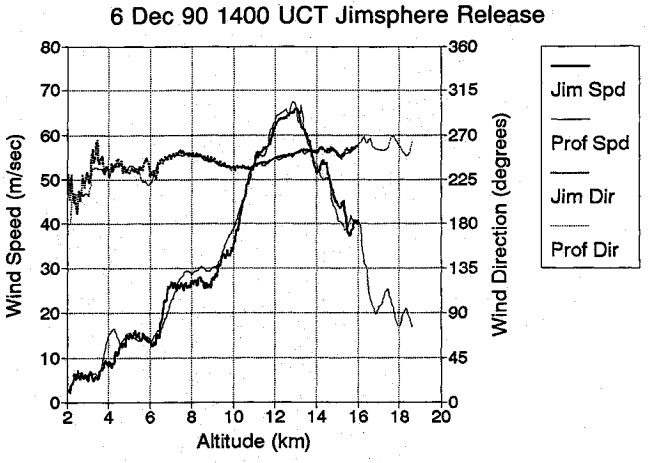

Fig. 9 Profiler and jimsphere wind profiles. Profiler data are from the 14:30 UCT median data.

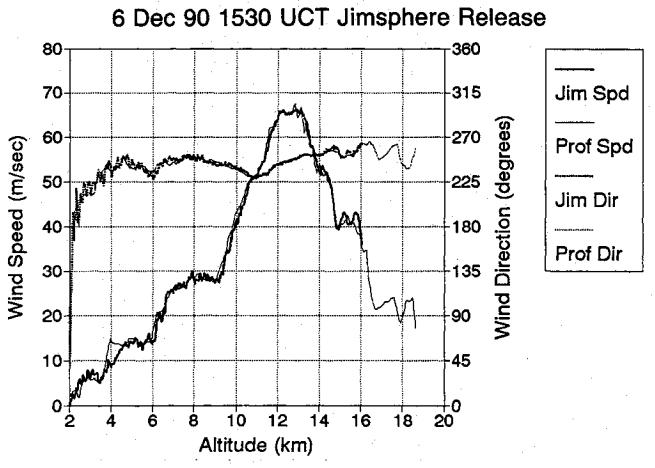

Fig. 10 Profiler and jimsphere wind profiles. Profiler data are from the 16:00 UCT median data.

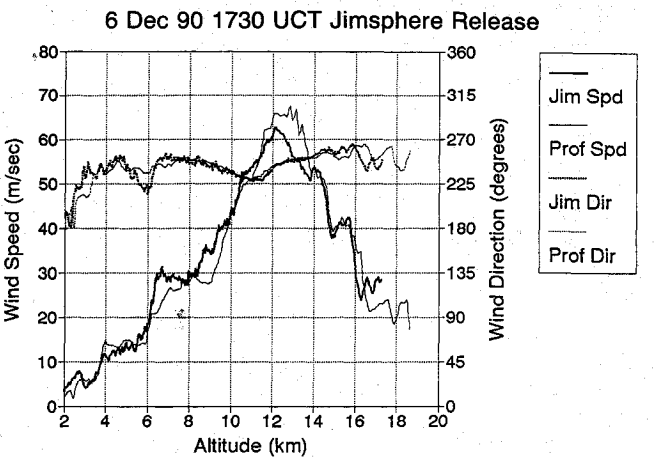

Fig. 11 Profiler and jimsphere wind profiles. Profiler data are from the 17:33 UCT median data.

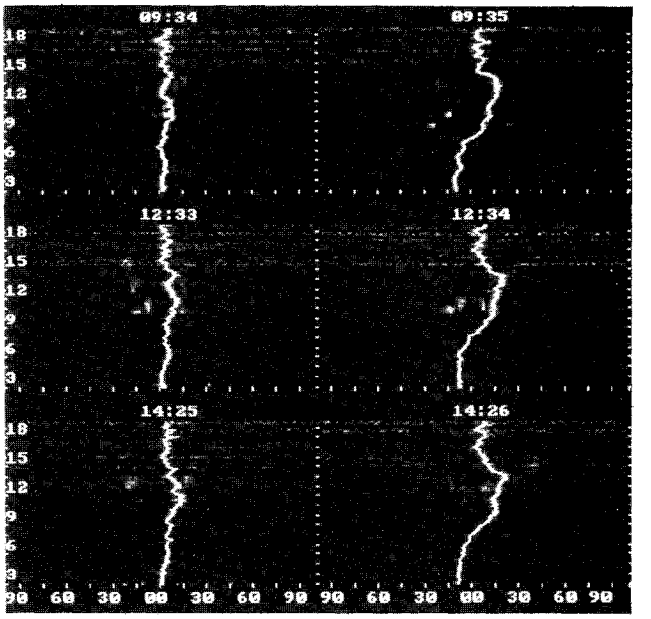

Fig. 12 Aug. 2, 1991 oblique beam power spectral profiles. See Fig. 4 for details.

In addition to this data display, there are, of course, a number of other potential quality control indicators available such as signal-to-noise ratios, spectral widths, vertical velocity profiles, as well as the first-guess propagation counter mentioned earlier.

Sample Data Sets

Once initiated, this technique can trace through very dynamic situations. To illustrate the performance, two sample data sets taken during very different synoptic regimes are shown.

One of our first spectral data sets extends from 14:06 UCT to 17:33 UCT on Dec. 6, 1990. This set is of particular interest because it demonstrates that the new technique performs well under unusual circumstances. During the time these data were taken, central Florida was under the influence of a continental polar air mass. Low temperatures were in the midforties, with highs in the midsixties. Aloft, centered at about 12 km was a strong subtropical jet stream with maximum speeds of 75–80 m/s. Near the center of the jet stream, the profiler signal-to-noise ratios were only occasionally above the minimum de-

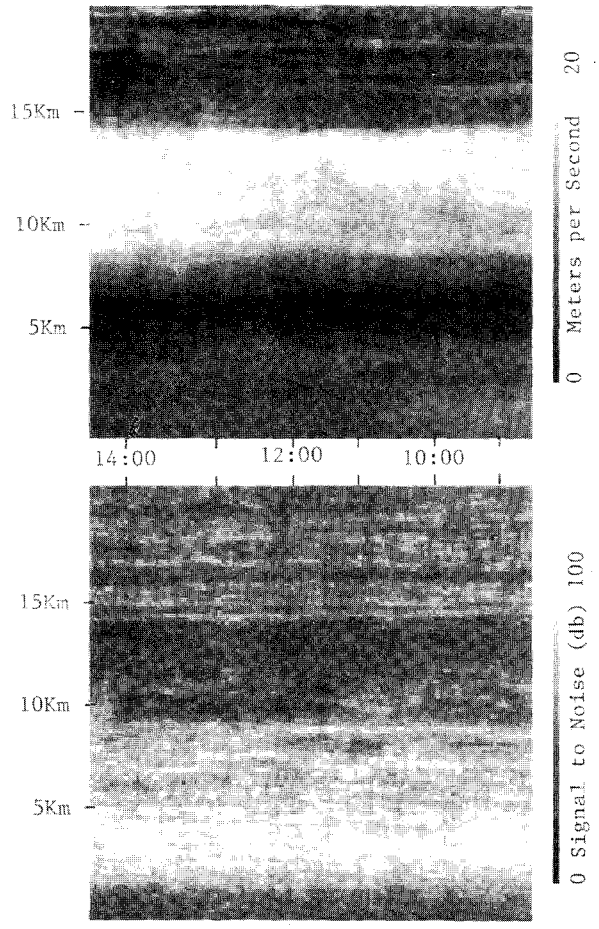

Fig. 13 Wind-speed (top) and signal-to-noise profiles from Aug. 2, 1991. Data are from 08:50 to 14:27 UCT. Time progresses from right to left. Signal-to-noise ratios have been corrected for range.

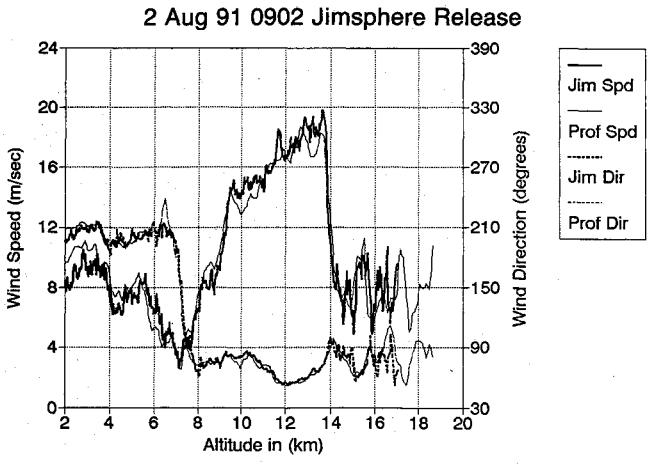

Fig. 14 Profiler and jimsphere wind profiles. Profiler data are from the 09:36 UCT median data.

tectable level until approximately 17:00 UCT. In addition, control units malfunctioned allowing the transmitter to operate at a slightly higher output than normal resulting in pronounced antenna ringing in the lower ten gates.

To commence processing on the data set, we formed the first guess by processing the 14:06 UCT spectral data using the standard, unenhanced software and visually correcting obvious errors. The low gate procedure was set to begin at gate 20 to accommodate the enhanced ringing. Following this initialization, the procedure was allowed to run using a three-point median spectral filter. No interaction to modify the first guess was needed during the processing of the 3.5 h data set.

Displaying the resulting data set in a concise form presents somewhat of a problem. Conventional wind barb displays become very cluttered if one attempts to present data from all gates on a single page. Instead, we summarize here in Fig. 8 by showing horizontal wind-speed time series as a gray scale display. In addition, Figs. 9–11 show jimsphere profiles from balloons released at 14:00 UCT, 15:30 UCT, and 17:30 UCT together with wind-profiler profiles corresponding approximately in time. Figure 8 also presents the signal-to-noise profiles for the vertical beam which can be used to help diagnose the location of features such as the jet stream core. Note the low signal-to-noise ratios that persist at approximately 12 km near the center of the jet stream.

The second data set presented here was taken during the launch of STS 39. At the time STS 39 was launched on August 2, 1991, the Bermuda high was strongly established with its axis extending into south central Florida. Weak southerly flow at low levels transitioned rapidly between 6–8 km to stronger easterly winds aloft.

Spectral data were taken from about 08:50 UCT until 14:27 UCT. Figure 12 shows samples of the three-point median filtered data without the velocity profile overlaid. These data correspond to the wind profiles presented in Figs. 14–16. Again to begin processing the data set, the first guess was formed by visual quality control of a wind profile produced by the standard processing method. Following the first-guess formulation, the complete data set was processed without manual intervention. Again we present the wind-speed profiles as a gray scale display together with the vertical beam signal-to-noise profiles in Fig. 13. Figures 14–16 show jimsphere and profiler velocity profiles corresponding approximately in time.

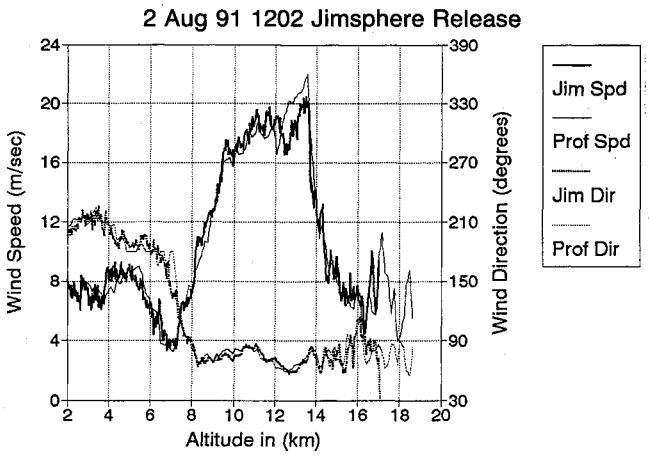

Fig. 15 Profiler and jimsphere wind profiles. Profiler data are from the 12:36 UCT median data.

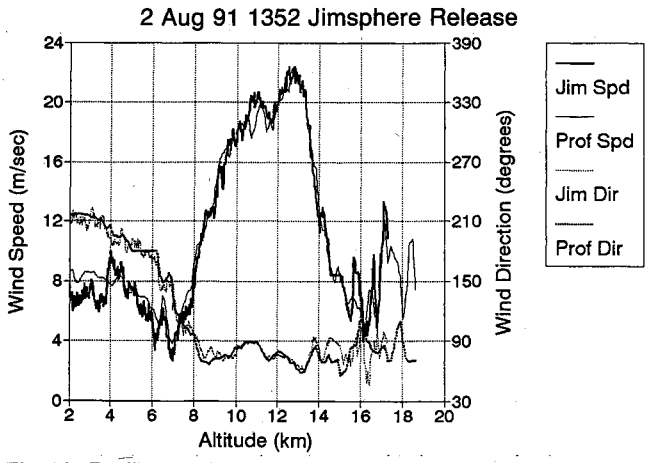

Fig. 16 Profiler and jimsphere wind profiles. Profiler data are from the 14:27 UCT median data.

Operational Considerations

Ultimately, one of the limiting factors in the operation of a vhf profiler such as the NASA prototype 50-MHz system is noise. The noise can be broken down into two components, system and external noise. The NASA 50-MHz system was designed to minimize system noise. Thus, the major noise source is the external or environmental noise. There are many different types of environmental noise detected by radars.[4] In Fig. 17, three common external noise sources have been identified. The first is the cosmic background noise which produces the minimum noise floor at all range gates during all collection times. The two maxima points occur when the profiler beams sweep through the galactic plane and receive radio-wave emissions from our Milky Way galaxy. The repeatable sequence of cosmic noise has a typical max-min range of about 7 dB as measured with the NASA radar. During normal operations, some signal loss may occur in the highest gates of the oblique beams during the short-lived cosmic maximum periods. It is unlikely that any loss will be found in the vertical beam because vertical beam signals benefit from a 6.5-dB reduction in the noise floor due to longer coherent integration times. Cosmic maxima periods occur at slightly different times in the three beams due to pointing differences. The 135-deg azimuth beam detects first, followed about 25 min later by the 45-deg azimuth beam, and about 45 min later by the vertical beam.

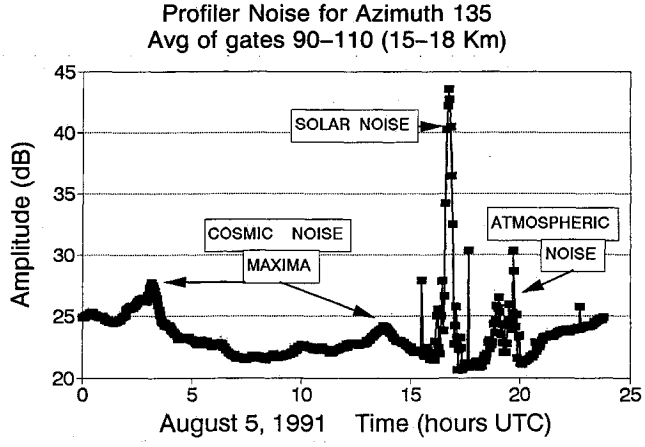

Fig. 17 Sample of profiler noise amplitude showing cosmic, solar, and atmospheric noise.

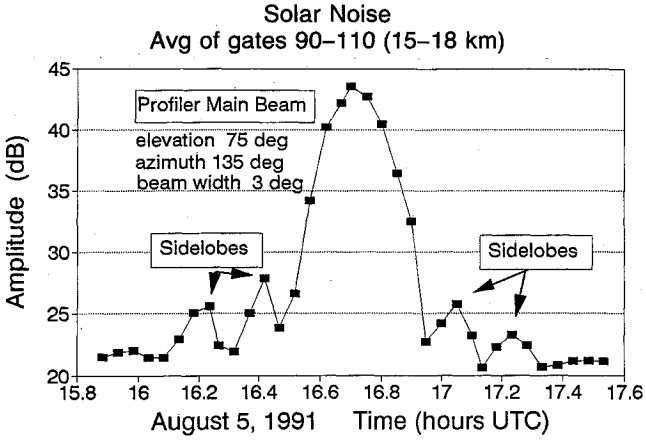

Fig 18 Solar Noise from Fig. 17.

A second type of broadband noise which is commonly found in this highly convective region of the United States is atmospheric noise associated with lightning. During the period from 18:00 UTC to 20:00 UTC, a cumulonimbus cloud formation was present in the vicinity of the profiler and lightning was frequently reported. Thus, the increase in the noise floor seen during this period can be assumed to be attributed to this phenomena. Other single 3-min period noise fluctuations seen in Fig. 17 are likely a result of man-made noise. There is a noticeable increase in noise fluctuations above the cosmic background during the day time hours at the Kennedy Space Center (KSC) which are likely related to urban noise.

The final noise type, solar noise, appears twice a year in the oblique 135-deg azimuth beam during May and August. Solar noise is by far the strongest noise source seen by the radar and it therefore can provide an opportunity for beam-pointing calibration. As a result of the solar noise intensity, radar beam sidelobes with amplitudes ranging from 3 to 6 dB above the noise floor are visible in Fig. 18. The Sun can have a significant, although short-lived effect on the collection of accurate velocity data. The noise floor in the 135-deg azimuth beam is raised sufficiently to obscure the atmospheric signals above about 9 km. The reduced signal-to-noise lasts for about 25 min during the days when the Sun passes through this beam.

Conclusions

We have found that a three-point median filter applied to successive spectral data effectively eliminates most spurious echoes from spectral data while improving signal-to-noise ratios. When combined with velocity calculations using a first guess, the result is a robust system that can extract high-quality wind profiles at 3-min intervals. As yet, we have not devised a completely automated quality control system. This does not, however, appear to be a significant shortcoming. The vertical continuity check done on each wind profile greatly reduces the probability of reporting an erroneous wind. We conducted extensive testing of the technique during the winter months of 1991–1992 on numerous data sets of lengths from 1–3 days. The technique was occasionally "fooled" by spurious signals in the spectra very near the atmospheric signal. In these cases, we found the effect lasted only for a few cycles and was obvious in the spectral data displays. During launch support operations, these spurious effects can be manually quality controlled using overlaid spectral data and velocity profiles.

References

[1]Clark, W. L., and Carter, D. A., "Real-Time Scaling of Atmospheric Parameters form Radars Using the MST Technique," *Proceedings of the 19th Conference on Radar Meteorology* (AMS, Miami Beach, FL), Jan. 1980, pp. 599–604

[2]Green, J. L., "An Example of Scaling MST Doppler Spectra, Spectral Smoothing, and Velocity Tracing," *Handbook for MAP,* Vol. 20, SCOSTEP Secretariat, Univ. of Illinois, Urbana, IL, 1986, pp. 472–475.

[3]Hildebrand, P. H., and Sekhon, R. S., "Objective Determination of the Noise Level in Doppler Spectra," *Journal of Applied Meteorology,* Vol 13, Oct. 1974, pp. 808–811.

[4]Skolnik, M. I., *Introduction to Radar Systems,* 2nd ed., McGraw-Hill, New York, 1980, pp. 461–464.

Alfred L. Vampola
Associate Editor